

---

# FRACTAL MANIFESTATIONS OF PERCOLATION-CLUSTER STRUCTURAL ELEMENT IN EMISSION SPECTRA OF SAMPLES WITH ZnSe QUANTUM DOTS

N.V. BONDAR

PACS 73.21.La, 78.67.Hc,  
78.55.Et  
©2011

Institute of Physics, Nat. Acad. of Sci. of Ukraine  
(46, Nauky Ave., Kyiv 03028, Ukraine; e-mail: [jbond@iop.kiev.ua](mailto:jbond@iop.kiev.ua))

---

Radiation by a percolation cluster of quantum dots has been detected for the first time, while studying dielectric specimens with ZnSe quantum dots, the concentration of which is both lower and higher than the corresponding percolation threshold. Different structural elements of the percolation cluster, such as the cluster backbone, dangling ends, and internal voids, were found to form their own bands in the specimen emission spectra. The excitonic state energy of each structural element was found to be mainly governed by the influence of the nearest neighbor elements, the amounts of which in the cluster backbone and the dangling ends are different. As a result, the corresponding excitonic states are resolved by energy and can be observed experimentally.

## 1. Introduction

In a biphasic system, where one phase is a continuous isotropic matrix, and the filling agent is represented by discrete inclusions of various shapes, there emerges a percolation phase transition of carriers (excitons), when the volume of inclusions achieves a certain critical value [1–6]. The corresponding percolation cluster consisting of inclusions provides the smearing of the exciton wave function, which is initially localized at separate inclusions, over a macroscopical distance, so that the properties of the biphasic system are changed; it is the well-known metal–insulator transition. The practical interest in studying the properties of the percolation cluster considered as a fractal object and the behavior of charge carriers in it is associated with the fact that the cluster structure reminds, on the whole, the structure of real materials, such as amorphous films, sensor systems, carbon nanotubes, and thick film resistors, which comprise the key elements of devices for nanophysics and optoelectronics [5, 6].

Although the structure of percolation clusters for lattice and continual (without any lattice) systems is well studied today theoretically [7–9], our understanding concerning the features of its formation in lattice-free sys-

tems remains at a low level. The main problem for such systems, which include the majority of real materials, as well as those examined in this work, is the determination of the critical filler volume  $\varphi_c$ , at which charge carriers (excitons) demonstrate a phase transition. The difficulty is that the transition can be stimulated by both the geometrical (classical) percolation of carriers [6], when the interaction between inclusions occurs immediately through a contact between their surfaces, as it takes place in certain granulated metals or composite mixtures, or the quantum-mechanical one, when the coupling between inclusions arises owing to the charge carrier tunneling. In both cases, contrary to the lattice systems, the  $\varphi_c$ -value can be determined only experimentally [1–4].

The formation of the percolation transition in specimens with metallic nanoparticles embedded into a dielectric matrix can be easily detected experimentally by monitoring a sharp growth of the specimen conductivity, when the volume occupied by nanoparticles reaches the  $\varphi_c$ -value [2–5]. It should be noted that, provided a considerable dielectric mismatch between the phases, the smaller is the nanoparticle radius, the smaller is the  $\varphi_c$ -value, at which the percolation transition arises [4]. A shortcoming of this experiment consists in that it does not allow the information concerning the structure of a percolation cluster to be obtained, but only fixes the time moment of the appearance of the cluster. The percolation cluster is known to be a fractal object. Therefore, it is not homogeneous and continuous, but a self-similar object characterized by the fractal dimensionality  $d_f \approx 2.54$  at distances  $\xi \sim |\varphi - \varphi_c|^{-\nu}$ , where  $\nu \approx 0.88$  [7–9]. The basis of the fractal cluster is a frame (or a backbone) with the dimensionality  $d_f^b \approx 1.86$ , which gives the main contribution to the specimen conductivity. At  $\varphi > \varphi_c$ , the percolation cluster has a significant number of internal voids of the dimension  $\xi$  and the so-called dangling ends connected with the backbone

by means of solitary bonds, which do not contribute to the specimen conductivity [9]. As a result, the voids and the dangling ends do not manifest themselves in the experiment, remaining a subject of theoretical studies at a computer simulation. Therefore, the specimens with metallic nanoparticles cannot be useful in studying the percolation cluster structure. In our opinion, the specimens with semiconducting quantum dots (QDs) at QD concentrations a little higher than the quantum-mechanical percolation threshold, when QDs do not form conglomerates yet, are the most suitable objects for this purpose.

In this work, with the use of specimens with ZnSe quantum dots, the concentrations of which are higher than the exciton percolation threshold, we have demonstrated that the structure of a percolation cluster manifests itself in the photoluminescence (PL) spectra generated not only by backbone exciton states (free states), but also by those, which are located in the cluster periphery or in the internal voids. We have also showed at the qualitative level that the energy mismatch between those states stems from different numbers of the nearest neighbors that surround a selected QD in the percolation cluster backbone and in the dangling ends or internal voids. We hope that the presented qualitative results will draw attention to this problem and obtain a serious theoretical substantiation.

## 2. Experimental Results

The technology for producing ZnSe quantum dots, their parameters, and optical spectra of specimens were published by us earlier [10–12]. In those works, on the basis of the corresponding analysis, we established the fact of the exciton percolation transition in a QD array and proposed a mechanism that explains this transition in the biphasic system with a substantial dielectric mismatch. However, the problem concerning the influence of the structure of the QD percolation cluster on the emission spectra of specimens with QDs was not considered. Therefore, it is the main goal of this work.

Let us present the major results in brief. In Fig. 1, the absorption spectrum of the matrix (the dashed curve) and the PL spectra of the studied specimens with ZnSe concentrations lower ( $x \approx 0.003\%$  and  $0.03\%$ ) and higher ( $x \geq 0.06\%$ ) than the exciton percolation threshold are depicted (see details in works [10, 11]). Curves 1 and 2 result from the recombination of heavy (hh) excitons, owing to the split of the degenerate valence band in ZnSe. As the amount of ZnSe in the matrix becomes larger, the curves undergo a red shift, and their inten-

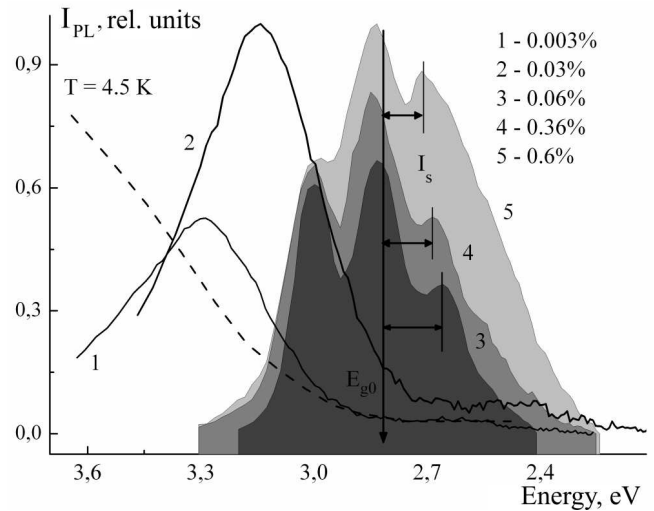


Fig. 1. Photoluminescence spectra registered under the excitation of specimens with various concentrations of ZnSe quantum dots by a He-Cd laser ( $\lambda = 325$  nm); the dashed curve is the absorption spectrum of the matrix without quantum dots

sities grow, owing to an increase of the average QD radius ( $R_0$ ) and the QD number in the matrix, respectively. The curves associated with light (lh) excitons are located considerably higher by energy than the curves associated with hh ones, which makes the registration of the former on our spectral device impossible. At the ZnSe concentration in the matrix  $x_c \approx 0.045\%$ , the emission spectrum (PL curves 1 to 3) drastically changes its shape. Further, its position becomes independent of the ZnSe amount in the matrix, but the intensities of PL bands continue to grow. The origin of this drastic modification lies in the realization of the percolation transition for excitons in the array of ZnSe quantum dots in the matrix [10–12]. As a consequence, the PL bands of hh and lh excitons become observable, as well as the long-wave band  $I_s$ , the nature of which was not considered in our previous works. In contrast to the lh and hh exciton bands generated by states in the percolation cluster backbone, we believe that the  $I_s$  band arises owing to the recombination of excitons captured at the dangling ends and in the internal voids of the cluster. The qualitative substantiation of this assumption and the nature of the  $I_s$  band will be given in the next section. Note that the spectral dependences of the lh, hh, and  $I_s$  bands on the ZnSe quantum dot concentration in the matrix,  $\rho$ , are different: unlike two first bands, the positions of which almost do not depend on  $\rho$ , the maximum of the  $I_s$  band undergoes a strong blue shift with respect to the hh exciton band,

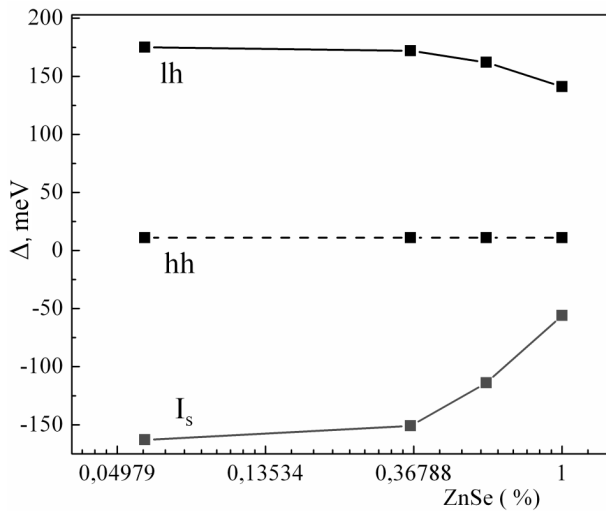


Fig. 2. Dependences of the lh exciton, hh exciton, and  $I_s$  band maxima on the ZnSe concentration (the quantum dot concentration) in the matrix

which is illustrated in Fig. 2, with a growth of its intensity.

In addition, Figs. 1 and 2 also demonstrate that, at the time moment, when the percolation cluster appears, the maximum of the  $I_s$  band is shifted by  $\Delta \approx 160$  meV with respect to the edge of the energy gap in crystalline ZnSe ( $E_{g0} = 2.82$  eV, denoted by an arrow). The spectral section, where the  $I_s$  band is located, corresponds usually in crystalline ZnSe to donor-acceptor pairs and excitons bonded at various impurity centers. According to the estimations in [13], QDs made of II-VI semiconductors and including about  $4 \times 10^3$  atoms contain 1 or 2 donor-acceptor pairs, which is a too low value for such an intensive band to be formed. Therefore, the source of this band should be sought evidently in the percolation cluster structure. Below, the qualitative explanation of this assumption is given.

### 3. Discussion of the Results Obtained

Before a discussion of the band  $I_s$  genesis, let us consider a diagram in Fig. 3, which gives a general idea of the formation and features of the percolation phase transition in our system. Figure 3,a exhibits a diagram representing a stochastic arrangement of ZnSe quantum dots with a certain dispersion of their dimensions in the matrix at a concentration lower than that, at which the level of exciton percolation through the system is formed. In this case, the majority of QDs preserve their individualities (black circles) and the quantum-mechanical dimensional

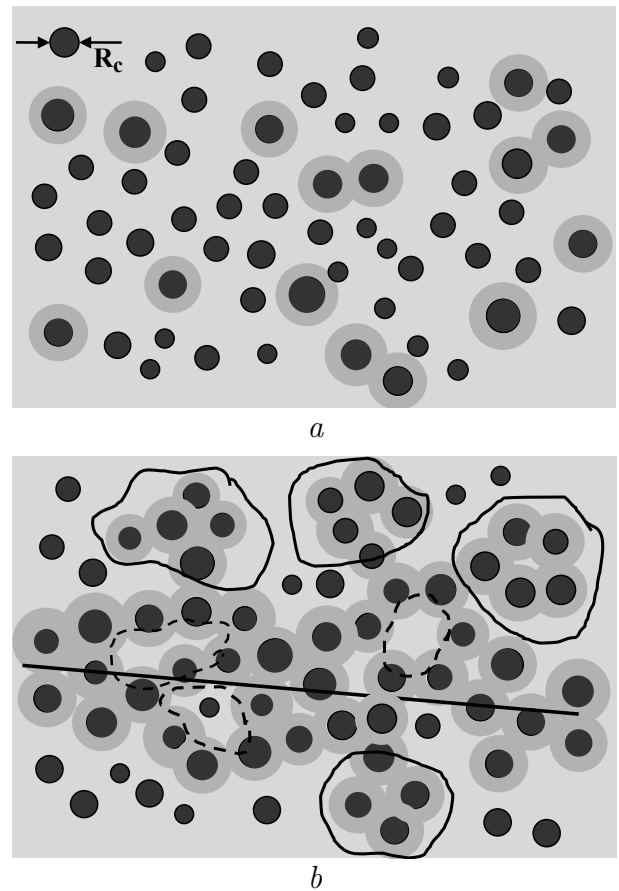


Fig. 3. Schematic representation of excitonic states in an array of quantum dots before (a) and after (b) the threshold. Black circles denote quantum dots with the spatial effect of excitons, and points with a gray shell correspond to quantum dots without the quantum effect, when one of the carriers is captured into an external polarization layer

state for excitons. However, because of the QD size dispersion, the radii of some of QDs exceeds the critical one (in our case,  $R_c \approx 30$  Å [10]), which results in the disappearance of the spatial effect of excitons in them and in the capture of either or both charge carriers into an external polarization well (dielectric trap) designated as a gray shell around a QD. Since the number of such QDs is small, they form solitary clusters or clusters composed of a few QDs. At  $\varphi \geq \varphi_c$ , a percolation cluster of coupled ZnSe quantum dots is formed (Fig. 3,b). In this case, the spatial effect of excitons disappears in the majority of QDs, which is a condition for the cluster to be formed. However, owing to the dispersion of QD dimensions, solitary QDs with  $R_0 < R_c$  still survive. As was indicated, the percolation cluster of ZnSe quantum dots has a fractal structure and is characterized by self-

similarity at distances of the order of  $\xi$ . At  $\varphi > \varphi_c$ , the quantity  $\xi$  is known to determine the size of internal cavities in the cluster.

The formed percolation cluster has an extremely loose structure with a large number of dangling ends and voids. Therefore, the cluster backbone contains only a small fraction of QDs [8, 9]. To demonstrate it, let us choose any point in the cluster and draw a sphere of radius  $r$  around it. Then, the number of QDs in it is  $N \sim (2r/L)^{d_f}$ , where  $L$  is the average distance between QDs in the percolation cluster. It is difficult to determine the value of  $L$  exactly. Therefore, it was chosen in the form [5]

$$L = D + d_0 = \left( \frac{\pi D^3}{6\varphi} \right)^{1/3}, \quad (1)$$

where  $D = 2R_c$ , and  $d$  is the distance between the surfaces of QDs. The number of QDs in the cluster backbone can be estimated by the formula

$$N_0 \approx \left( \frac{2r}{L_0} \right)^{d_f^b}, \quad (2)$$

where  $L_0$  is the average distance between the nearest neighbors in the cluster backbone (we determined it in works [10, 11]), whence  $L/L_0 \approx 1.7$ .

Let us estimate the ratio  $N/N_0$  in a section of the percolation cluster, by assuming the dimension of an exciting laser spot  $r = 50 \mu\text{m}$ , which is natural in our case. Selecting the corresponding fractal dimensions [9], we obtain  $N/N_0 \approx 200$ , which testifies that the main part of the percolation cluster is presented by its dangling ends. The sizes of internal voids in a percolation cluster can be evaluated as follows:  $\xi \approx L_0 |\varphi - \varphi_c|^{-0.88} \approx 2.5 \times 10^3 \text{ \AA}$ , where  $\varphi_c \approx 0.08$  [10, 11]. The voids together with the dangling ends of the cluster form a large number of non-radiative centers. Therefore, the intensity of the  $I_s$  band is lower than that of the hh band formed by the cluster backbone. This is also confirmed by the dependence of the  $I_s$  band intensity on the temperature. Namely, the intensity decreases much quicker than that of the hh exciton band at a small temperature increment [10, 11]. The growth of the ZnSe quantum dot concentration in the matrix gives rise to a simultaneous increase of the numbers of QDs in the backbone and dangling ends of the percolation cluster. The number of QDs in the dangling ends increases much quicker, because the QD clusters with finite dimensions join the percolation cluster, which results in an accelerated growth of the  $I_s$  band in comparison with the hh or lh exciton bands. At the same time, the dimensions  $\xi$  and, accordingly, the number of

nonradiative decay channels for excitons get smaller. As a result, a considerable growth of the PL intensity for the hh and  $I_s$  bands is observed (Fig. 1, curve 5), which confirms the made assumption.

The most difficult task of this section is the explanation of the spectral position of the  $I_s$  band with respect to  $E_{g0}$  or the maximum of the hh exciton band. From Figs. 1 and 2, one can see that, in the as-formed percolation cluster, the difference  $\Delta = E_{g0} - I_s \approx 160 \text{ meV}$  decreases, as the number of QDs in the matrix increases. Let us name the quantity  $\Delta$  as the binding energy of the excitonic state in dangling ends reckoned from the exciton energy in the backbone.

It is easy to understand the dependence of  $\Delta$ -value on the QD concentration in the matrix, which is shown in Fig. 2. In the percolation cluster backbone, every QD is surrounded by QDs, whose number is minimally  $n_1 = 2.7$  and maximally  $n_2 = 12$ : the first number is no more than a minimal number of bonds per QD for the threshold exciton percolation to emerge, the second one is the maximum number of QDs with radius  $R_0$  needed to cover the surface of a QD of the same size. Hence, the excitonic state energy in a selected QD depends, besides other factors, also on the number of neighboring QDs: the more this number, the more is the energy; it is a situation typical of a QD in the cluster backbone. On the contrary, in selected QDs located in the cluster dangling ends, the number of neighbors is low ( $n < n_1$ ); therefore, the excitonic energy levels at such QDs fall within the forbidden gap of the percolation cluster. An increase in the number of QDs in the matrix mainly affects the structure of cluster dangling ends, the QD concentration in which grows; the number of neighbors increases for every QDs, and, as a result, the  $\Delta$ -value decreases (Fig. 2). Unfortunately, there are no works till now, in which the theoretical calculations of the excitonic state energy have been carried out for a configuration, when the hole is in a QD and the electron is captured in an external polarization well, being coupled with it by the Coulomb interaction. It is also true for the influence of neighboring QDs on this state. This influence would manifest itself in that the  $\Delta$ -value should start to decrease, which is observed in our case.

However, some qualitative estimates can be made. For example, we can determine the binding energy  $\varepsilon_x$  of an exciton under the condition  $R_0 \rightarrow \infty$ , i.e. the plane state energy, when an electron is located in the matrix (glass) and coupled with the ZnSe surface by means of image forces. As was shown in work [14], there exists at least one electron energy level in such a one-dimensional

potential,

$$\varepsilon_x = \frac{1}{2} \frac{m_e^* e^4}{4\hbar^2 \varepsilon_2} \left( \frac{\varepsilon_1 - \varepsilon_2}{\varepsilon_1 + \varepsilon_2} \right)^2, \quad (3)$$

where  $m_e^* = 0.5m_0$  is the effective mass of an electron in glass, and  $\varepsilon_1 = 9.25$  and  $\varepsilon_2 = 2$  are the dielectric constants of ZnSe and the matrix, respectively. The quantity  $\varepsilon_x$  is the upper limit with respect to that of a spherical surface. The distance from the electron to the ZnSe surface is determined by the formula [14]

$$b = \frac{3}{2} \frac{2\hbar^2 \varepsilon_2}{m_e^* e^2} \left( \frac{\varepsilon_1 + \varepsilon_2}{\varepsilon_1 - \varepsilon_2} \right). \quad (4)$$

Substituting the relevant values, we obtain that  $\varepsilon_x \sim 340$  meV and  $b \approx 16$  Å. The hole, which is on the other side of this interface, induces the surface polarization, the sign of which coincides with the hole charge sign, so the hole has to be repulsed from the interface. However, its Coulomb interaction with the electron stabilizes the exciton. Therefore, taking this interaction into account, we obtain  $\varepsilon_x \sim 400$  meV. Hence, since  $\varepsilon_x > \Delta \approx 160$  meV, this quantity really is the upper limit for an exciton in a spherical QD. An increment in the number of QDs in the matrix leads to an increase of the numbers of QDs in both the cluster backbone and its periphery. However, in the former case, this leads to a simple growth of the hh exciton band intensity, whereas, in the latter case, to an increase of the neighbor number for a selected QD in the dangling end; this gives rise to a reduction of  $\Delta$ , which is observed in Figs. 1 and 2, and confirms, in general, the qualitative model proposed above.

To summarize, by studying the specimens with ZnSe quantum dots in a dielectric matrix, in which the QD concentration is higher than the percolation threshold, the low-temperature PL spectra, whose shape is governed by the radiation of excitons locating in various structural elements of the percolation cluster (the backbone, dangling ends, and internal voids), have been registered for the first time. It is found experimentally that the energy of excitons in separate QDs, which are located in different cluster elements, depends on the number of their neighbors. However, no theoretical calculations of such a dependence have been made till now. We hope that the qualitative results obtained will draw attention to this problem, because it is interesting from not only theoretical, but also practical viewpoints.

1. K.S. Deepa, M.T. Sebastian, and J. James, Appl. Phys. Lett. **91**, 202904 (2007).
2. K.S. Deepa, S.K. Nisha, P. Parameswaran, M.T. Sebastian, and J. James, Appl. Phys. Lett. **94**, 142902 (2009).
3. J.I. Hong, L.S. Schadler, and R.W. Siegel, Appl. Phys. Lett. **82**, 1956 (2003).
4. Q.Q. Yang and J.Z. Liang, Appl. Phys. Lett. **93**, 131918 (2008).
5. Jing Li and Jang-Kyo Kim, Com. Scien. Tech. **67**, 2114 (2007).
6. N. Johnner, C. Grimaldi, I. Balberg, and P. Ryser, Phys. Rev. B **77**, 174204 (2008).
7. V. Blavatska and W. Janke, Phys. Rev. Lett. **101**, 125701 (2008).
8. I.M. Sokolov, Usp. Fiz. Nauk **150**, 221 (1986).
9. D. ben-Avraham and Sh. Havlin, *Diffusion and Reactions in Fractals and Disordered Systems* (Cambridge Univ. Press, Cambridge, 2000).
10. N.V. Bondar and M.S. Brodyn, Physica E **42**, 1549 (2010).
11. N.V. Bondar and M.S. Brodyn, Fiz. Tekh. Poluprovodn. **44**, 915 (2010).
12. N.V. Bondar, Fiz. Nizk. Temp. **35**, 307 (2009).
13. V.A. Fonoberov, K.A. Alim, and A.A. Balandin, Phys. Rev. B **73**, 165317 (2006).
14. B.V. Perepelitsa, Fiz. Tekh. Poluprovodn. **3**, 2328 (1969).

Received 20.06.11.

Translated from Ukrainian by O.I. Voitenko

ПРОЯВИ СТРУКТУРНИХ  
ЕЛЕМЕНТІВ ПЕРКОЛЯЦІЙНОГО  
КЛАСТЕРА ЯК ФРАКТАЛЬНОГО  
ОБ'ЄКТА У СПЕКТРАХ ВИПРОМІНЮВАННЯ  
ЗРАЗКІВ З КВАНТОВИМИ ТОЧКАМИ ZnSe

М.В. Бондар

Резюме

Під час дослідження зразків з квантовими точками ZnSe в діелектричній матриці з концентраціями нижче та вище порога перколяції екситонів, вперше виявлено випромінювання з перколяційного кластера квантових точок як фрактального об'єкта і встановлено, що різні структурні елементи такого кластера, а саме, остов (хребет), мертві кінці та внутрішні порожнини формують свої смуги спектра фотолюмінесценції зразків. Показано, що енергія екситонних станів кожного структурного елемента кластера зумовлена, головним чином, впливом найближчих сусідів, кількість яких є різною у хребті кластера і на його периферії, в результаті чого екситонні стани рознесені по енергії і можуть спостерігатись в експерименті.